

pH-sensitive doxorubicin-loaded polymeric nanocomplex based on β -cyclodextrin for liver cancer-targeted therapy

This article was published in the following Dove Medical Press journal:
International Journal of Nanomedicine

Tianfeng Yang^{1,*}

Guowen Du^{2,*}

Yuxin Cui¹

Runze Yu¹

Chen Hua²

Wei Tian^{2,3}

Yanmin Zhang¹

¹School of Pharmacy, Health Science Center, Xi'an Jiaotong University, Xi'an, Shaanxi 710061, China;

²The Key Laboratory of Space Applied Physics and Chemistry Ministry of Education and Shanxi Key Laboratory of Macromolecular Science and Technology, School of Science, Northwestern Polytechnical University, Xi'an 710072, China; ³Xi'an Institute for Biomedical Materials and Engineering, Northwestern Polytechnical University, Xi'an 710072, China

*These authors contributed equally to this work

Background: Doxorubicin (DOX) is one of the most effective treatments for hepatocellular carcinoma (HCC), but is restricted by its poor pharmacokinetics. Herein, we exploited efficient targeted drug delivery systems and they have been found to be a worthy strategy for liver cancer therapy.

Materials and methods: We investigated polymeric nanoparticles which were synthesized based on host-guest interaction between β -cyclodextrin and benzimidazole. The properties of nanoparticles with regard to size/shape, encapsulation efficiency, and drug release were investigated using conventional experiments. Cell proliferation assay in vitro, cell uptake assay, and cell apoptosis analysis were used to investigate cytotoxicity, uptake, and mechanism of targeted supramolecular prodrug complexes (TSPCs)-based self-assemblies and supramolecular prodrug complexes (SPCs)-based self-assemblies.

Results: The pH-sensitive lactobionic acid (LA)-modified pH-sensitive self-assemblies were synthesized successfully. The results of in vitro released assay showed that the accelerated release of DOX from TSPCs-based self-assemblies with the decrease of pH value. When TSPCs-based self-assemblies were taken up by HepG2 cells, they demonstrated a faster release rate under acidic conditions and proved to have higher cytotoxicity than in the presence of LA. A mechanistic study revealed that TSPCs-based self-assemblies inhibited liver cell proliferation by inducing cell apoptosis.

Conclusion: The pH-sensitive nanocomplex, as liver-targeted nanoparticles, facilitated the efficacy of DOX in HepG2 cells, offering an appealing strategy for the treatment of HCC.

Keywords: pH-sensitive, hepatocellular carcinoma, doxorubicin, drug delivery

Introduction

Cancer is a major public health problem worldwide and is the second leading cause of death.¹ Hepatocellular carcinoma (HCC) is a prevalent liver malignancy with poor prognosis and accounts for 85%–90% of all primary liver cancers.² Chemotherapy, as one of the most effective treatment methods for HCC, is still used as the frontline approach in clinics,³ for instance doxorubicin (DOX), which can inhibit the synthesis of DNA and RNA.⁴ However, one major handicap of DOX is the systemic distribution in normal tissue of patients because of its poor pharmacokinetics.⁵ Based on this situation, nanotechnologies are appealing because they can facilitate a combined effect, which is commonly used in HCC therapy.⁶ Many efficient drug delivery systems with all kinds of biomaterials have been designed to reduce severe side effects including micelles,⁷ liposomes,⁸ macromolecules,⁹ supramolecular polymers, etc.¹⁰ Among these classes of carriers, supramolecular polymer-based carriers have attracted considerable attention because of their excellent biocompatibility and structural versatility.¹¹ β -cyclodextrin

Correspondence: Wei Tian
Xi'an Institute for Biomedical Materials and Engineering, Northwestern Polytechnical University, 127 Youyi West Street, Xi'an, Shaanxi 710072, China
Email happytw_3000@nwpu.edu.cn

Yanmin Zhang
School of Pharmacy, Health Science Center, Xi'an Jiaotong University, 76 Yanta West Street, 54, Xi'an, Shaanxi 710061, China
Email zhang2008@mail.xjtu.edu.cn

(β -CD) is regarded as an important kind of supramolecular system, which is the commonest host compound, exhibiting good complexation capacities with all kinds of hydrophobic drugs.¹² The property of β -CD indicates that it can be used as functional delivery system by means of molecular recognition and self-assembly. As early as 1994, the first report of β -CD-based supramolecular hydrogel proved its potential application in the field of nanomedicine.¹³ Benzimidazole and its derivatives are important materials and intermediate products, which can self-assemble with β -CD by host-guest interaction.

In the meantime, because of the intense demands for intelligent drug delivery systems, more and more multifunctional drug carriers have been exploited, such as those possessing features like temperature-, pH-, ultrasound-, light-sensitivity etc.^{14–18} And, worth mentioning, is that tumor cells have a lower pH than normal cells because of anaerobic glucose metabolism in tumor cells,¹⁹ so the pH-triggered approach is one of the most efficient tactics for anti-tumor drug delivery systems, which is expected to stabilize the drug in the natural environment. For instance, the chitosan-coated mixed micellar nanocarriers loaded with DOX and siRNA were used to provide pH responsiveness, and the nanocomplexes showed better DOX release in acidic tumor pH environments.²⁰ In addition, many tumor cells have specific expression of numerous receptors which are very important for malignant tumor proliferation, such as folate receptor²¹ and biotin receptor.²² Particularly in HCC, the galactose and N-acetyl-galactosamine-terminated glycoproteins are recognized by asialoglycoprotein receptor (ASGPR) located on the surface of liver cancer cells,²³ hence ASGPR-mediated targeted delivery system has been regarded as one of the most efficient methods for treating HCC. Nowadays, several galactose-containing ligands including lactobionic acid (LA) have been used for hepatocyte-targeted drug delivery.²⁴ As an endogenous molecule possessing wonderful biocompatibility,²⁵ LA has great advantages in modifying nanoparticles for liver cancer therapy.

In this research, we developed a targeted prodrug based on host-guest interaction containing benzimidazole for pH-sensitivity. The host molecule β -CD and targeted molecule LA were coupled with polyethylene glycol (PEG) successively by alkylation and click reaction. We had a hypothesis that targeted supramolecular prodrug complexes (TSPCs)-based self-assemblies possess good biocompatibility and PEG could prolong the half-life of the prodrug in vivo. Meanwhile, the object-chain segment, benzimidazole modified DOX (BM-DOX), was synthesized from benzimidazole via a three-step reaction including esterification, hydrazination, and hydrazone formation. The hydrazone bond was expected to be cleaved

in the intracellular acidic environment with rapid release of DOX from the prodrug,^{26,27} resulting in enhanced inhibition of cellular proliferation. Finally, β -CD-modified PEGylated LA (LA-PEG- β -CD) and BM-DOX were assembled with each other to form a self-assembled polymer by host-guest interaction,²⁸ and the supramolecular force inside these complexes resulted in nanoscale self-assemblies (Scheme 1). The TSPCs- and supramolecular prodrug complexes (SPCs)-based self-assemblies were synthesized and characterized by regular characterization methods. Besides, the pH-sensitive release of DOX from prodrug was investigated under different pH conditions. Finally, the tumor cell inhibition properties of TSPCs- and SPCs-based self-assemblies were tested through cell culture of human hepatoma HepG2 cells in vitro.

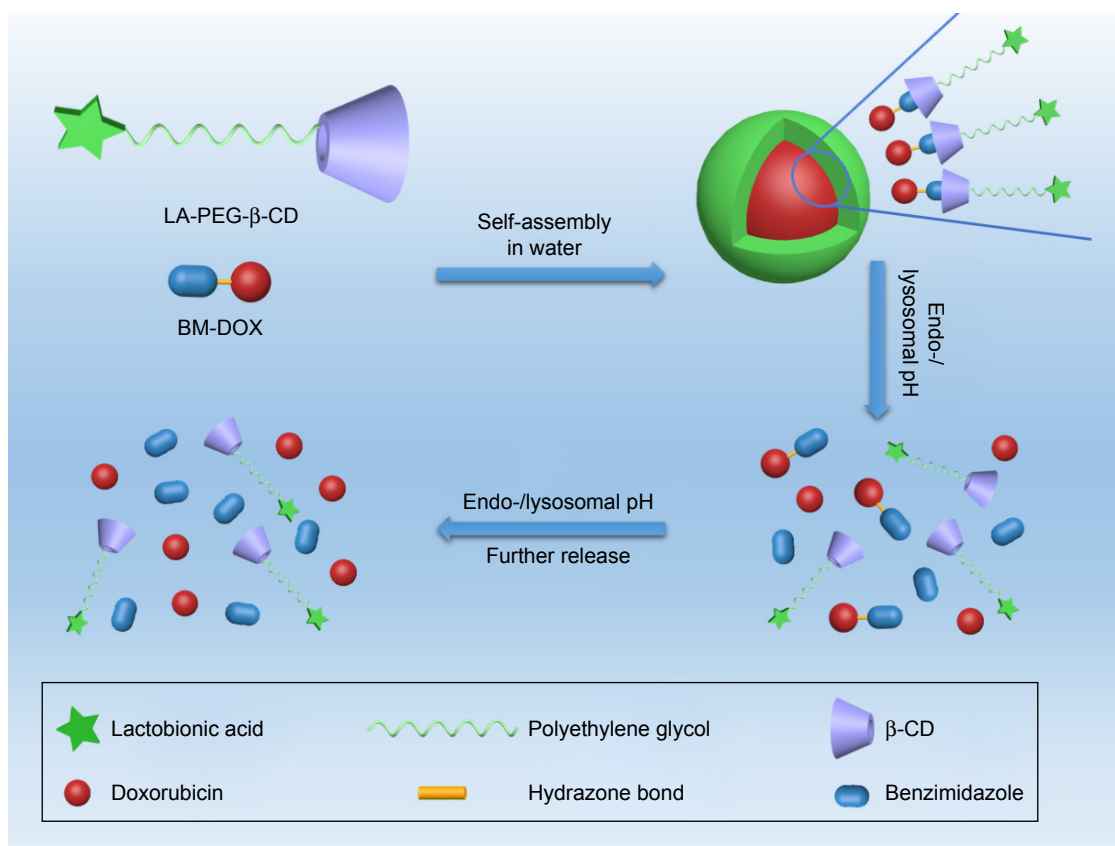
Materials and methods

Materials

For details of the main chemical reagents, please refer to the [Supplementary materials](#). DMEM, RPMI-1640 medium, and PBS were obtained from HyClone (Logan, UT, USA). FBS was purchased from ExCell Bio (Shanghai, China). Trypsin-EDTA solution and Penicillin-Streptomycin solution, 100X were acquired from Solarbio Science & Technology Co., Ltd (Beijing, China). MTT, DMSO, propidium iodide (PI), and Hoechst 33258 were obtained from Sigma-Aldrich Co. (St Louis, MO, USA). LA was purchased from Shanghai Aladdin Biochemical Technology Co., Ltd. (Shanghai, China). Annexin V-fluorescein isothiocyanate FITC reagent kit was purchased from KeyGen Biotech Inc (Nanjing, China). Human normal liver cells L02 (GNHu6), human non-small-cell lung cancer cells A549 (TCHu150), and human liver cancer cells HepG2 (TCHu72) were purchased from Shanghai Institute of Cell Biology, Chinese Academy of Sciences (Shanghai, China). All other reagents used were of analytical grade. A549 cells were cultured in RPMI-1640 medium with 10% FBS (v/v), L02 and HepG2 cells were cultured in DMEM with 10% FBS (v/v). All cell lines were maintained in an incubator with a humidified atmosphere of 5% CO₂ at 37°C.

Preparation of TSPCs- and SPCs-based self-assemblies

The subject-chain segment, LA-PEG- β -CD and PEGylated β -CD (mPEG- β -CD) were obtained by substitution reaction and click reaction. And object-chain segment (BM-DOX) was synthesized by successive esterification, hydrazination, and hydrazone formation. The specific routes, which can be referred to, were shown in [Scheme S1–S5](#) in the [Supplementary materials](#). In order to obtain TSPCs- and SPCs-based self-assemblies, 5 mg of LA-PEG- β -CD was



Scheme 1 Schematic illustration of preparation, proposed degradation mechanism of TSPCs-based self-assemblies, and consequent release of DOX.

Abbreviations: BM-DOX, benzimidazole modified DOX; β-CD, β-cyclodextrin; DOX, doxorubicin; LA-PEG-β-CD, β-CD-modified PEGylated LA; PEG, polyethylene glycol; TSPCs, targeted supramolecular prodrug complexes.

dissolved in 2 mL deionized water, then 1 mg of BM-β-CD was added into the solution. The mixture was constantly stirred for 6 hours at room temperature after being exposed to ultrasound for 10 minutes to accelerate molecular diffusion, which was critical for uniformity during host–guest interaction. TSPCs- and SPCs-based self-assemblies were collected via dialysis (molecular weight cut off: 1,000 D) in water for 6 hours and lyophilization. The dialysate containing the BM-DOX was evaluated by means of UV-visible spectrophotometry after acidification. Subtraction method was implemented as follows: the amount of drug in dialysate was subtracted from the total amount and fitted into the calibration equation of DOX solution (Figure S1) to calculate drug loading capacity (DLC) and drug loading efficiency (DLE).

$$\text{DLC (\%)} = \frac{\text{Amount of drug in self-assemblies}}{\text{Amount of self-assemblies}} \times 100\% \quad (1)$$

$$\text{DLE (\%)} = \frac{\text{Amount of drug in self-assemblies}}{\text{Total amount of drug in feed}} \times 100\% \quad (2)$$

All polymer precursors were well-defined and characterized by ^1H spectroscopy, ^{13}C nuclear magnetic resonance (NMR) spectroscopy, ^1H - ^1H nuclear Overhauser effect spectroscopy (NOESY), and Fourier transform infrared spectroscopy.

Particle size and zeta potential analysis

The particle size and zeta potential analysis were conducted by means of Malvern Zetasizer Nano ZS at 25°C. TSPCs- and SPCs-based self-assemblies were suitably dissolved in deionized water or PBS, and diluted to a final concentration of 1 mg/mL. HCl and NaOH were used in treatment of acidification and alkalization, respectively. The average size and zeta potential of samples were evaluated by dynamic light scattering (DLS) and laser Doppler microelectrophoresis at room temperature, respectively.

Transmission electron microscopy (TEM)

The TEM images used to assess size and morphology were obtained with Hitachi H-7650 transmission electron microscope at an acceleration voltage of 80 kV. Samples were diluted to 1 mg/mL, and were prepared by dropping

10 μ L of polymer solution on the copper grids. The polymer settled on the copper grids under static condition for a few minutes before aqueous solution was removed with filter paper. The samples were then counter-stained with phosphotungstic acid and dried at room temperature for testing.

In vitro release study of TSPCs-based self-assemblies

Dialysis method was the main way to realize the release study in vitro. The study was performed in PBS of different pH values. An amount of 15 mg of freeze-dried TSPCs-based self-assemblies was dissolved in 7.5 mL deionized water, and 2.5 mL solution was added into a dialysis bag (MWCO 500). Then, three dialysis bags were soaked in a glass bottle containing 30 mL of release medium with different pH values at 37°C under continuous shaking (110 rpm). At each pre-determined time point, 3 mL of the release medium was withdrawn from the bottle for characterization. Meanwhile, the same volume of fresh buffer solution was added to the bottle to maintain the total volume. The amount of DOX in each sample was evaluated by UV-2550 (Shimadzu, Japan) spectroscopy (the excitation wavelength was 485 nm [Figure S2]), and could be calculated with the aid of calibration curve of DOX. The total amount of released DOX was calculated using the following formula, and averaged from three repeated measurements.

$$\text{Cumulative release (\%)} = \frac{100 \left(30.0C_n + 3.0 \sum C_{n-1} \right)}{W_0} \quad (3)$$

C_n and C_{n-1} are the concentration of DOX determined by UV spectrometry for the n_{th} time and the $(n-1)_{th}$ time to take 3 mL dialyzate as sample from glass bottle respectively, W_0 is the total amount of DOX, at $t=0$, present in the dialysis bag.

Cell proliferation assay

The biocompatibility of materials and the effect of self-assemblies were detected by MTT assay. L02, HepG2, and A549 cells were seeded in 96-well plates in complete medium and cultivated overnight. Then, the cells were treated with different treatments at final DOX concentrations of 1, 3, 5, 7, and 10 μ g/mL for 48 hours. To test the liver target of TSPCs-based self-assemblies, HepG2 cells were incubated with LA at a concentration of 100 μ g/mL for 1 hour. Meanwhile, to investigate the pH-sensitivity of self-assemblies, SPCs- and TSPCs-based self-assemblies were pretreated

with PBS (pH =5.0) for 1 hour. After treatment, cells were cultured with serum-free medium and MTT (5 mg/mL) for 4 hours, followed by the addition of 150 μ L DMSO for 15 minutes. The absorbance was measured using a microplate reader (Bio-Rad Laboratories Inc., Hercules, CA, USA) at a wavelength of 490 nm. Three independent experiments were performed.

Cell uptake assay

Exponentially growing cells were seeded in 6-well plates at a density of 2×10^5 cells per well. After incubating for 24 hours, the cells were treated with different treatments at a final DOX concentration of 5 μ g/mL for 12 hours. Then, the cells were harvested and the cell suspension was collected in a 1.5 mL Eppendorf tube, and washed with PBS three times followed by centrifugation at 1,000 rpm for 5 minutes at 37°C. Then, the cells in each tube were suspended by the addition of 400 μ L PBS. The DOX content in the cells was detected and analyzed by FACS (ACEA Novocyte, San Diego, CA, USA).

Exponentially growing cells were seeded in 96-well plates at a density of 2×10^4 cells per well. After incubating for 24 hours, the cells were washed with PBS three times after removing the medium. Then, the cells were fixed in 4% paraformaldehyde for 15 minutes at room temperature. Then, cells were washed with PBS and stained with DAPI in the dark at room temperature for 10 minutes. Images were obtained using an inverted fluorescence microscope (DM505, Nikon Corporation, Tokyo, Japan).

Flow cytometric analysis of cell apoptosis

A549 and HepG2 cells were plated in 6-well plates in complete medium and cultivated overnight. Then, cells were treated with indicated treatments at a final DOX concentration of 5 μ g/mL for 24 hours. Then cells were harvested, washed with PBS, and subjected to sequential staining with 5 μ L Annexin V-FITC. After 5 minutes, 10 μ L PI (20 μ g/mL) was added and cells were incubated in the dark, at room temperature for 10 minutes. All stained cells were analyzed by FACS (ACEA Novocyte).

Hoechst staining assay

Tumor cells were seeded in 12-well plates at a density of 4×10^5 cells per well and then treated with different treatments for 24 hours. Cells were washed with PBS and fixed with 4% paraformaldehyde for 10 minutes. Then, cells were washed with PBS and stained with Hoechst 33258 in the dark, at room

temperature for 20 minutes. Images were obtained using an inverted fluorescence microscope (DM505).

Results and discussion

Synthesis of SPCs and TSPCs

To obtain TSPCs and SPCs, building blocks including LA-PEG- β -CD and BM-DOX were first synthesized by click reaction and Schiff-base reaction, according to the routes shown in [Schemes S1–S5](#) in the [Supplementary materials](#). All polymer precursors were well-defined and characterized, and the data were provided in [Figures S3–S12](#). SPCs and TSPCs were then constructed through host–guest interaction between mPEG- β -CD/LA-PEG- β -CD and BM-DOX in aqueous solutions, respectively. NMR spectra of SPCs and TSPCs ([Figures 1 and S13](#)) were firstly utilized to confirm the formation of host–guest complexes. [Figure 1A](#) shows the 2D NMR NOESY spectra of an equimolar solution of LA-PEG- β -CD (4 mmol/L) and BM-DOX (4 mmol/L) in D_2O at 25°C, which indicated that the signals of BM protons were correlated with those of inner protons in β -CD. The signals at δ 6.9–7.4 ppm attributed to the BM moieties of BM-DOX show cross-peaks, resulting from dipolar interactions with the signals at 3.5–4.0 ppm ascribed to the H-3 and H-5 protons located within the cavity of β -CD moieties in

LA-PEG- β -CD. This phenomenon proved that BM moieties were deeply embedded within the β -CD cavities. Similarly, the 2D NMR NOESY spectra of SPC solutions ([Figure 1B](#)) revealed the appearance of the correlation peaks between the protons of BM and the inner protons of β -CD, indicating the formation of host–guest complexes.

Size and morphology of TSPCs- and SPCs-based self-assemblies

The self-assembly behaviors of SPCs and TSPCs in aqueous solutions were studied by DLS and TEM. The average size of SPCs-based self-assemblies was 27 ± 1 nm while the size of TSPCs-based self-assemblies obviously increased to 68 ± 3 nm due to the introduction of LA ([Figure 2A and B](#)). Furthermore, TEM images revealed clear spherical morphology in both SPCs- and TSPCs-based self-assemblies, and the sizes observed in TEM images were consistent with the results determined by DLS ([Figure 2C and D](#)). It should be noted that, the morphology of TSPCs-based self-assemblies was not uniformly distributed and the size was much larger than those of SPCs-based self-assemblies. A reasonable explanation is that charged groups like LA and amino acid may have had some effects on the properties of self-assemblies or complexes such as size and zeta potential.²⁹

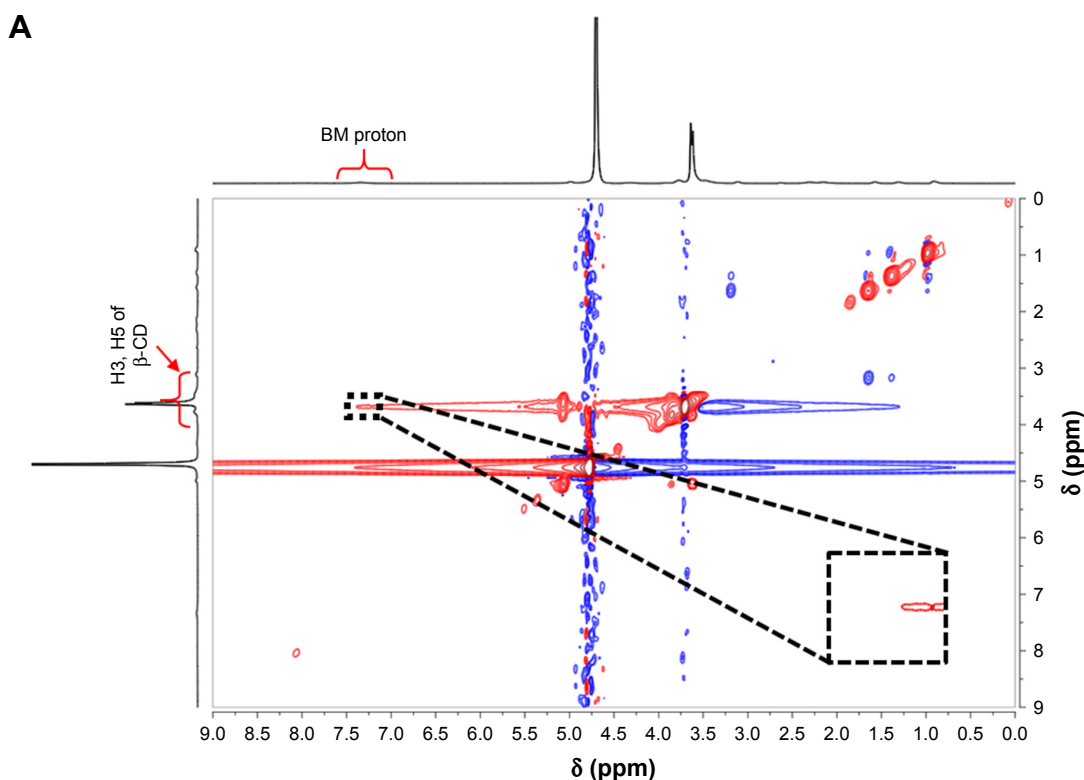


Figure 1 (Continued)

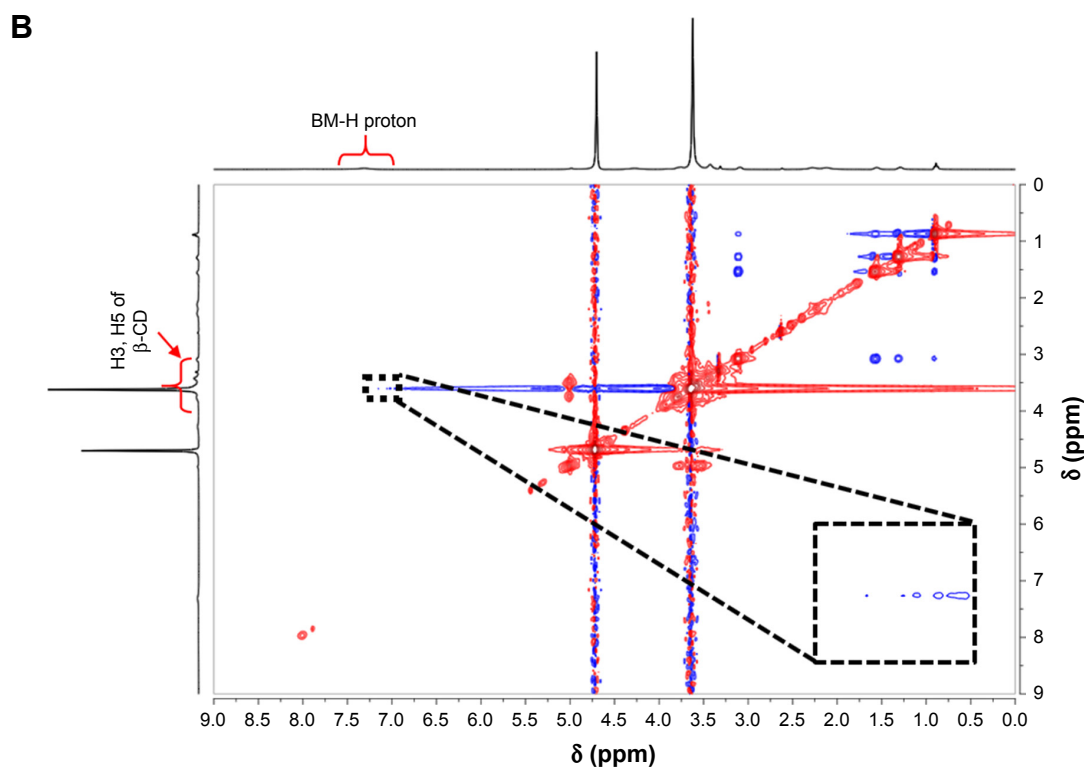


Figure 1 2D NOESY NMR spectra of TSPCs-based self-assemblies and SPCs-based self-assemblies.

Note: 2D NOESY NMR spectra of TSPCs- (A) and SPCs-based self-assemblies (B) in 0.5 mL D₂O (inset: partial enlargement).

Abbreviations: β-CD, β-cyclodextrin; BM, benzimidazole modified; NMR, nuclear magnetic resonance; NOESY, nuclear Overhauser effect spectroscopy; SPCs, supramolecular prodrug complexes; TSPCs, targeted supramolecular prodrug complexes.

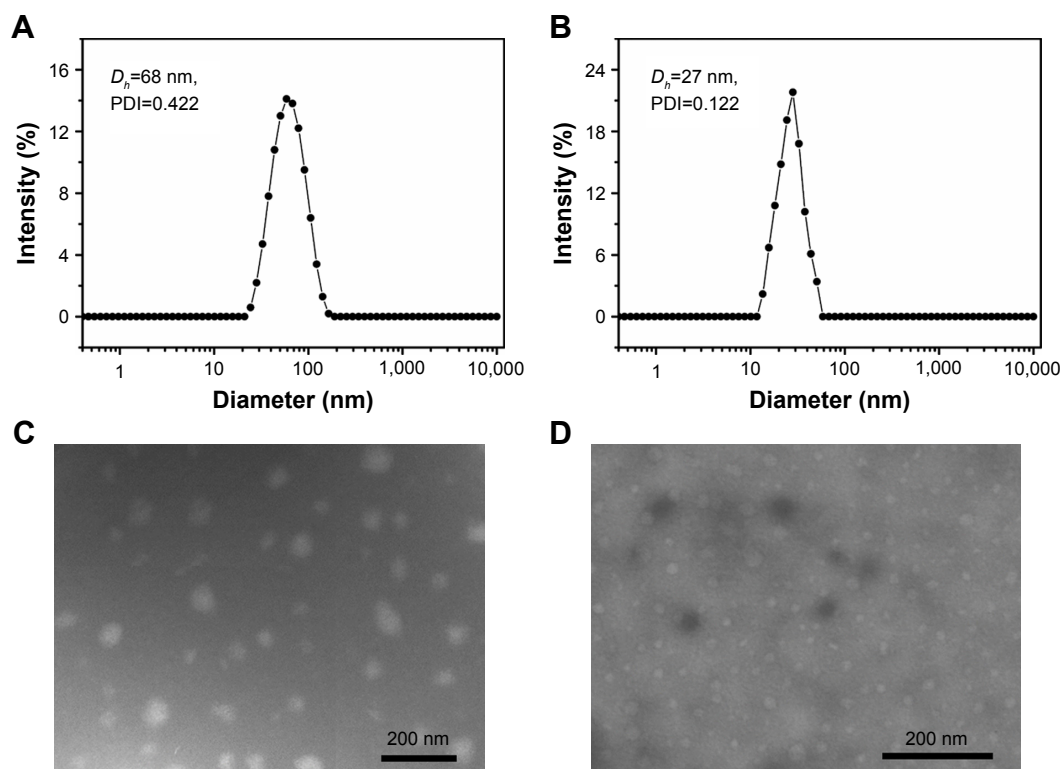


Figure 2 Physicochemical characterization of TSPCs- and SPCs-based self-assemblies.

Notes: Particle size distribution of TSPCs-based self-assemblies (A) and SPCs-based self-assemblies (B). TEM images of TSPCs-based self-assemblies (C) and SPCs-based self-assemblies (D).

Abbreviations: PDI, polydispersity index; SPCs, supramolecular prodrug complexes; TEM, transmission electron microscopy; TSPCs, targeted supramolecular prodrug complexes.

pH-responsive reversibility of SPCs- and TSPCs-based self-assemblies

As we know, host–guest interactions between β -CD and BM can be cleaved under acidic conditions, leading to disassembly and subsequent drug release.^{30,31} The pH-triggered reversibility of TSPCs- and SPCs-based self-assemblies upon

acid stimulus was further investigated by DLS and UV-visible spectrophotometry. In Figure 3A, the hydrodynamic diameter (D_h) value of TSPCs-based self-assemblies changed from 68 ± 3 nm to 18 ± 2 nm under acidic environment due to the protonation of BM, because the exclusion of the water-soluble BM from the hydrophobic inner cavity of β -CD would lead

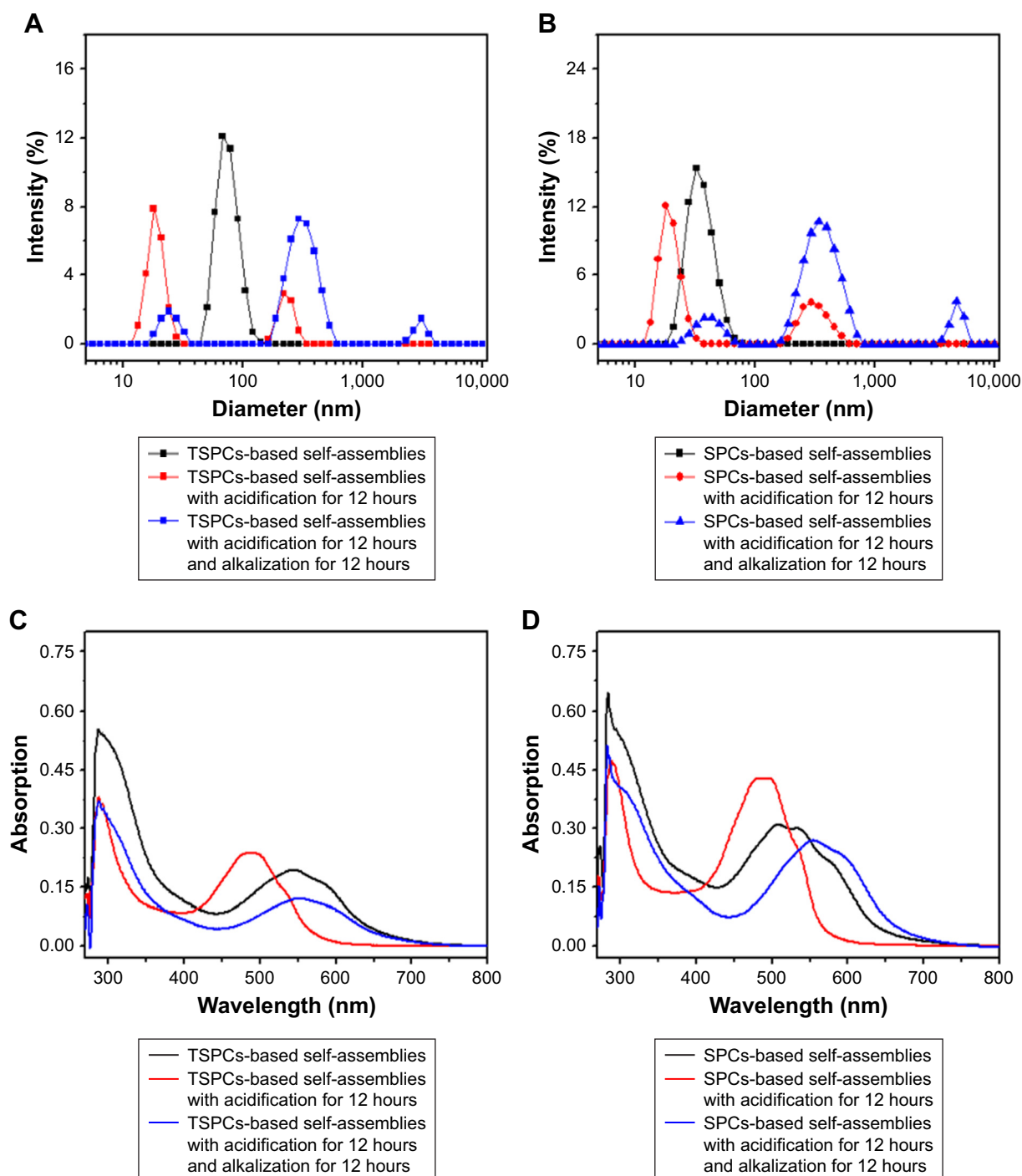


Figure 3 Redox-triggered reversibility confirmation of TSPCs- and SPCs-based self-assemblies in deionized water.

Notes: Particle size distribution of TSPCs-based self-assemblies (A) and SPCs-based self-assemblies (B); initial state (black line), after acidification for 12 hours (red line), and after acidification for 12 hours and alkalization for 12 hours (blue line). UV-visible absorption spectra of TSPCs-based self-assemblies (C) and SPCs-based self-assemblies (D); initial state (black line), after acidification for 12 hours (red line), and after acidification for 12 hours and alkalization for 12 hours (blue line).

Abbreviations: SPCs, supramolecular prodrug complexes; TSPCs, targeted supramolecular prodrug complexes.

to the dissociation of microsphere.³¹ The subsequent alkali additive led to an increase in size to hundreds of nanometers, indicating the pH-induced reversibility of TSPCs-based self-assemblies. Similarly, the same phenomenon observed as the reversible process was confirmed in SPCs-based self-assemblies solution (Figure 3B).

UV-visible absorption spectra also confirmed the pH-triggered reversible feature of TSPCs- and SPCs-based self-assemblies. In Figure 3C, compared with λ_{\max} =544 nm of initial absorbance, the corresponding λ_{\max} absorbance of DOX decreased to 485 nm upon acidification for 12 hours because DOX was released from self-assemblies and exposed to the solution owing to the destruction of self-assemblies under acidic condition. With subsequent alkalization for 12 hours, the λ_{\max} absorbance of DOX increased from 485 nm to 553 nm. According to the data shown in Figure S2 (λ_{\max} =541 nm of DOX's absorbance in alkaline solution), the red shift of λ_{\max} of absorption of TSPCs-based self-assemblies in alkaline condition indicated the formation of reversible dynamic covalent bonds (hydrazone bond) which could affect the absorbance of DOX, which has been reported by Gao et al.³² There was a similar occurrence in SPCs-based self-assemblies, as shown in Figure 3D.

Stability of TSPCs-based self-assemblies

As a promising prodrug, the favorable ability to maintain size fluctuation within a controlled range is a critical property.³³ Thus, the size and zeta stability of TSPCs-based self-assemblies were further evaluated via real-time DLS testing in pH 7.4 PBS. As shown in Figure 4, TSPCs-based self-assemblies were fairly stable and maintained a constant size of 70 nm in PBS, and only a slight fluctuation was observed within 1 month. Additionally, the zeta potential of TSPCs-based self-assemblies presented

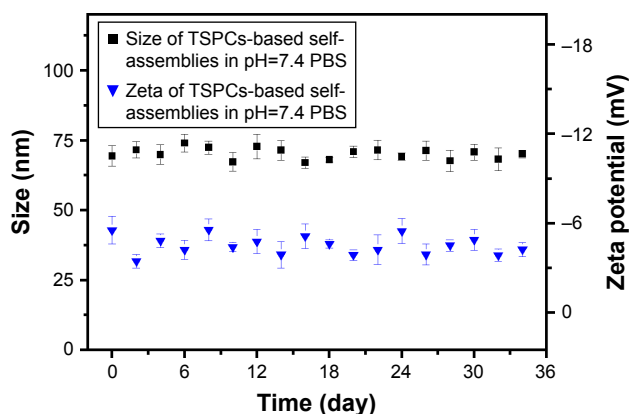


Figure 4 Size stability testing of TSPCs-based self-assemblies.

Note: Change tendency of size and zeta potential within approximately 1 month.

Abbreviation: TSPCs, targeted supramolecular prodrug complexes.

similar stability and maintained a potential of -4.46 mV. Nano-prodrugs with diameter larger than 200 nm are known to induce non-specific scavenging by monocytes and the reticuloendothelial system.³⁴ Hence, these results indicated that TSPCs-based self-assemblies may possess prolonged circulation time and enhance tumor accumulation in vivo.

Controlled drug release of TSPCs-based self-assemblies in vitro

The DLC and DLE of TSPCs-based self-assemblies were 11.74% and 12.96% determined by aforesaid subtraction method, respectively. The drug release study was performed in pH 6.0, pH 7.4 (corresponding to the normal blood environment), and pH 5.0 (simulating the pH in mature endosomes of tumor cells) PBS, as shown in Figure 5A.³⁵ It could be observed that the accelerated release of DOX was obvious with the decrease in pH value. What is more, the sustained release of the loaded DOX from TSPCs-based self-assemblies indicated that the relatively hydrophobic dendrimer interior could prevent the drug's burst release.³⁶ Specifically, TSPCs-based self-assemblies displayed a fairly slow DOX release rate in pH 7.4 PBS, and 21.41% of DOX was released within 24 hours. In contrast, 83.38% of DOX was released from TSPCs-based self-assemblies in pH 5.0 PBS at the same time. The amount of DOX released in pH 6.0 PBS was between that of pH 5.0 and pH 7.0, reaching 53.45% within 24 hours. These results indicated that an acidic environment could accelerate the breakdown of self-assemblies, further giving rise to faster release of the drug. As stated previously, benzimidazole could be protonated in an acidic environment, resulting in the dissociation of host-guest interaction. Furthermore, an acidic environment caused the cleavage of hydrazone bond and decomposition of the hydrophobic block to release DOX molecules from TSPCs-based self-assemblies.³⁷ The release mechanism of DOX from TSPCs-based self-assemblies was thus proposed to elucidate the release behavior by studying the release kinetics with a simple semi-empirical equation (Equation 3) and a modified equation (Equation 4) to describe the release behavior.³⁸

$$\frac{M_t}{M_\infty} = kt^n \quad (4)$$

$$\ln r = \ln k + n \ln t, \dots r = \frac{M_t}{M_\infty} \quad (5)$$

M_t and M_∞ are the cumulative amounts of guest molecule released at time t and infinity, respectively; k is the release constant; and n describes the kinetic and release mechanism.

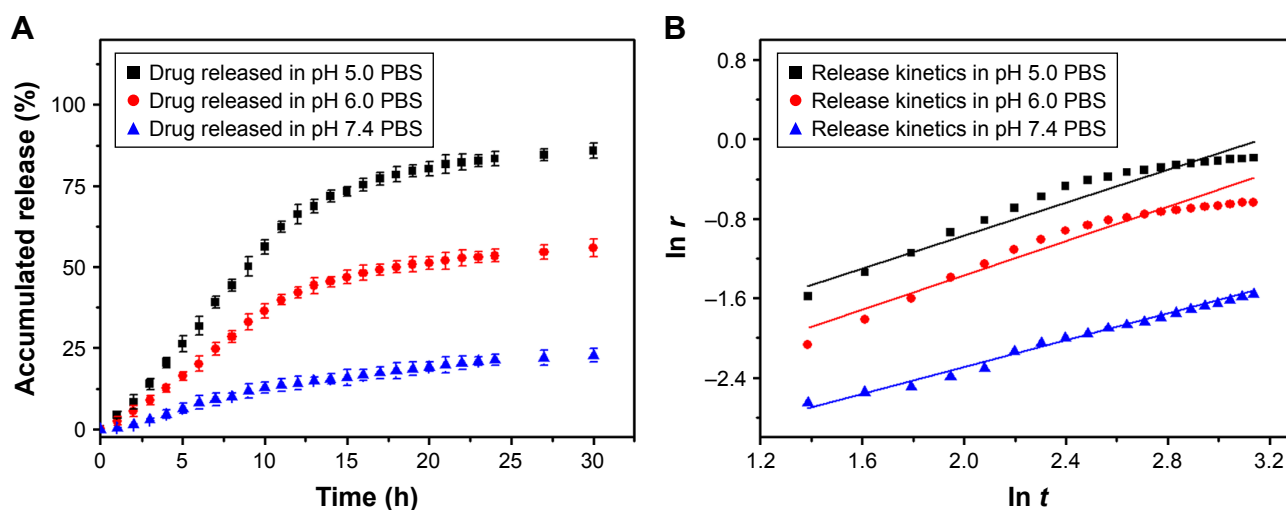


Figure 5 Time-dependent release of DOX from TSPCs-based self-assemblies.

Notes: (A) Cumulative release curves of DOX from TSPCs-based self-assemblies as a function of time over a period of 30 hours in PBS with different pH values at 37°C. (B) Corresponding fitted curves for release kinetics. All quantitative data represent mean \pm SD ($n=3$).

Abbreviations: DOX, doxorubicin; SPCs, supramolecular prodrug complexes; TSPCs, targeted supramolecular prodrug complexes.

For spherical particles, n is usually between 0.43 and 0.85. When n is close to 0.43, diffusion, referred to as “Fickian diffusion”, is the major driving force. When n is close to 0.85, the release is mainly controlled by degradation.³⁹ As was shown in Figure 5B and Table 1, the cumulative release amount and release time of DOX from TSPCs-based self-assemblies exhibited a linear correlation during the test time at 37°C. As a result of n value being close to 0.85, the release mechanism of DOX in an acidic condition was mainly dominated by degradation. In particular, n values decreased from 8.2–6.5 with the increase of pH value from 5.0–7.4. The phenomenon indicated that the dominance of the degradation mechanism increased to a greater extent for TSPCs-based self-assemblies when exposed to an acidic environment due to the effect of hydrazination and β -CD/BM binding sites.

Biocompatibility and cytotoxicity of SPCs- and TSPCs-based self-assemblies

The biocompatibility of drug-free self-assemblies is of crucial importance for the further use of materials as drug

carriers. Herein, the biocompatibility of self-assemblies was investigated using normal liver cells L02, human non-small-cell lung cancer cells A549, and human liver cancer cells HepG2, by MTT assay. As shown in Figure 6A, the drug-free self-assemblies did not show cytotoxicity against L02, A549, and HepG2 cells even if the concentration of polymers was 200 $\mu\text{g/mL}$, indicating that the biocompatibility of the materials used for drug carriers is decent. Additionally, MTT assay was conducted to detect the targeting and pH-responsiveness of SPCs- and TSPCs-based self-assemblies in vitro, the results indicated that TSPCs-based self-assemblies showed more toxicity than SPCs-based self-assemblies on HepG2 cells instead of A549 cells (Figure 6B and C). Furthermore, to verify the TSPCs-based self-assemblies' uptake through LA receptors, a competitive inhibition experiment was conducted in the presence of free LA (100 $\mu\text{g/mL}$). The cytotoxicity was decreased and there was no distinct difference between the two self-assemblies (Figure 6C), which suggested that the free LA competed with TSPCs-based self-assemblies for LA receptor binding sites. Moreover, when the polymers were pretreated in PBS solution (pH=5.0), which was used to mimic tumor microenvironment conditions, for 1 hour, as shown in Figure 6D and E, SPCs- and TSPCs-based self-assemblies could further inhibit tumor cell proliferation, which could be due to the acidic environment which facilitated the release of DOX. All these results revealed that TSPCs-based self-assemblies have liver cancer-targeting and pH-responsiveness features, hence, it can be used as drug carrier and targeting agent for liver cancer therapy.

Table 1 Release kinetics parameters of DOX from TSPCs-based self-assemblies in PBS with different pH values at 37°C fitted with Peppas³⁶ formula^a

pH	Fitting equation	n^b	k^b	R^{2b}
5.0	$\ln r = -0.827 \ln t - 2.625$	0.827	0.072	0.939
6.0	$\ln r = -0.794 \ln t - 2.970$	0.794	0.051	0.932
7.4	$\ln r = -0.657 \ln t - 3.612$	0.657	0.027	0.991

Notes: ^aAll experiments were conducted at 37°C. ^bCalculated by using Equation 4.

Abbreviations: DOX, doxorubicin; TSPCs, targeted supramolecular prodrug complexes.

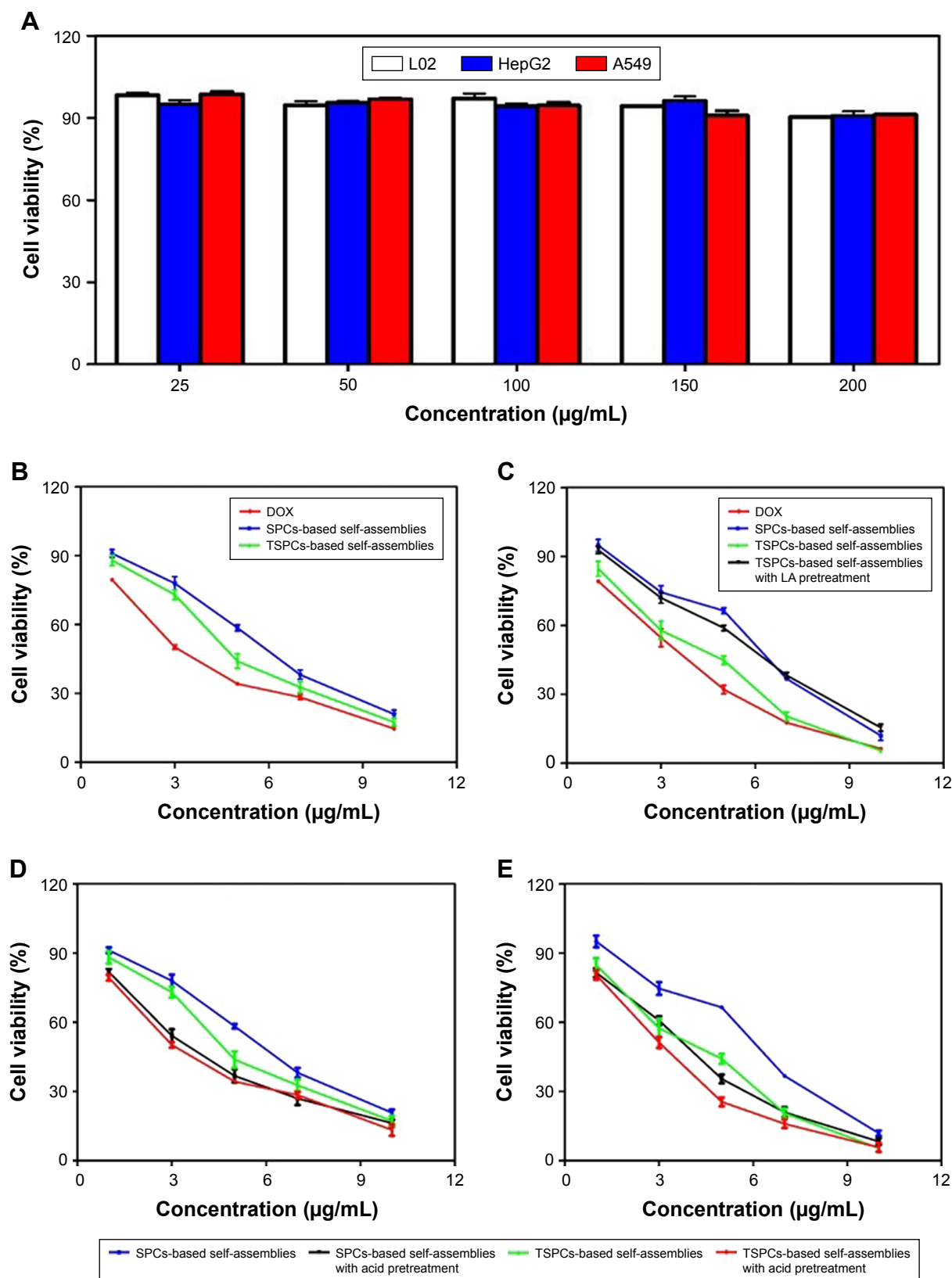


Figure 6 Biocompatibility and cytotoxicity of TSPCs- and SPCs-based self-assemblies.

Notes: (A) Effect of drug-free self-assemblies in L02, A549, and HepG2 cells. (B, C) Effect of free DOX, TSPCs-based self-assemblies in the absence or presence of free LA for 1 hour and SPCs-based self-assemblies at final DOX concentrations of 1, 3, 5, 7, 10 µg/mL in A549 (B) and HepG2 (C) cells. (D, E) Effect of SPCs- and TSPCs-based self-assemblies pretreated in PBS solution (pH =5.0) for 1 hour in A549 (D) and HepG2 (E) cells. Data were expressed as mean \pm SD (n=5).

Abbreviations: DOX, doxorubicin; LA, lactobionic acid; SPCs, supramolecular prodrug complexes; TSPCs, targeted supramolecular prodrug complexes.

Cellular uptake of SPCs- and TSPCs-based self-assemblies

A major requirement for the therapeutic efficacy of drugs is cellular uptake efficiency.⁴⁰ To further confirm the host-guest interaction-enhanced adjustable release of DOX from TSPCs-based self-assemblies, we evaluated the cellular uptake behavior with flow cytometry and by using an inverted fluorescence microscope. Flow cytometry analysis indicated that only the HepG2 cells treated with TSPCs-based self-assemblies had the same high fluorescence signal compared with the cells treated with free DOX after 12 hours' co-culture

(Figure 7A and B). In addition, the competitive inhibition was investigated using flow cytometry in the presence and absence of free LA by measuring the fluorescence intensity of DOX. As shown in Figure 7B, the fluorescence intensity of DOX was decreased in the presence of free LA after 1 hour of incubation, which confirmed that TSPCs-based self-assemblies were taken up via LA receptors. To comparatively investigate the intracellular internalization of free DOX, SPCs-, and TSPCs-based self-assemblies by A549 and HepG2 cells, we further carried out a fluorescence-based localization study using an inverted fluorescence microscope – the stained cell

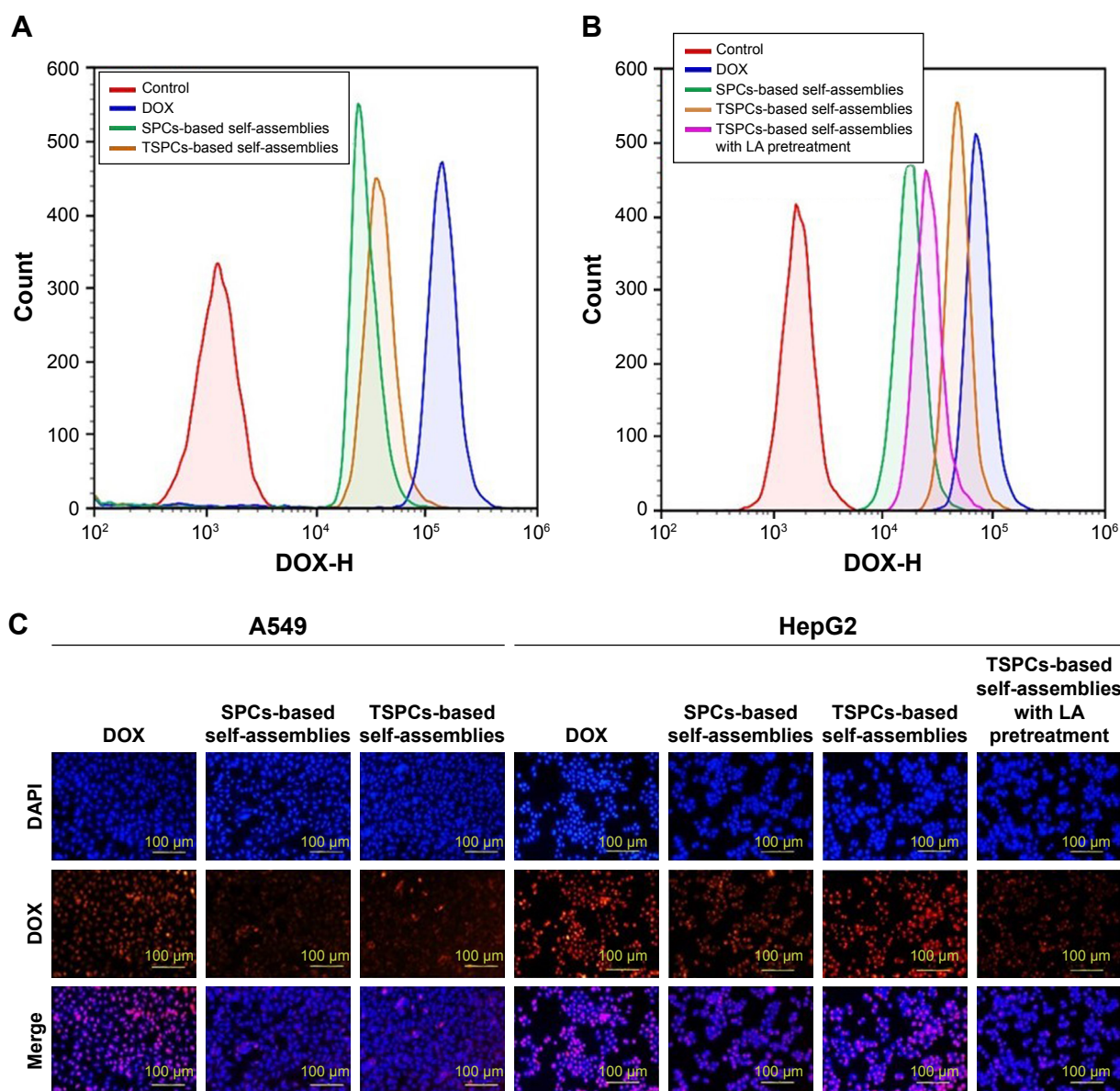


Figure 7 Cellular uptake and intracellular distribution of TSPCs- and SPCs-based self-assemblies.

Notes: (A, B) The DOX fluorescence signal of A549 (A) and HepG2 (B) cells after being treated with TSPCs- or SPCs-based self-assemblies for 12 hours at a final DOX concentration of 5 μ g/mL. (C) Photographs of A549 and HepG2 cells stained with DAPI (blue) and incubated with DOX (red); cells were incubated with TSPCs- or SPCs-based self-assemblies at a final DOX concentration of 5 μ g/mL for 12 hours.

Abbreviations: DOX, doxorubicin; LA, lactobionic acid; TSPCs, targeted supramolecular prodrug complexes.

nuclei and DOX showed a blue and red fluorescence. As shown in Figure 7C, the DOX fluorescence intensity could clearly be observed in both the cytoplasm and nuclei of HepG2 cells after 12 hours' incubation with TSPCs-based self-assemblies, while free DOX mainly appeared in the nucleus, which may be correlated to the slow release of DOX in self-assemblies compared with free DOX. Moreover, the

DOX fluorescence signal in the HepG2 cells was significantly reduced in the presence of free LA, which further confirmed that the TSPCs-based self-assemblies were taken up through LA receptors in HepG2 cells. In summary, the results were consistent with the results obtained by flow cytometry, which demonstrated that TSPCs-based self-assemblies could be internalized by liver cancer cells.

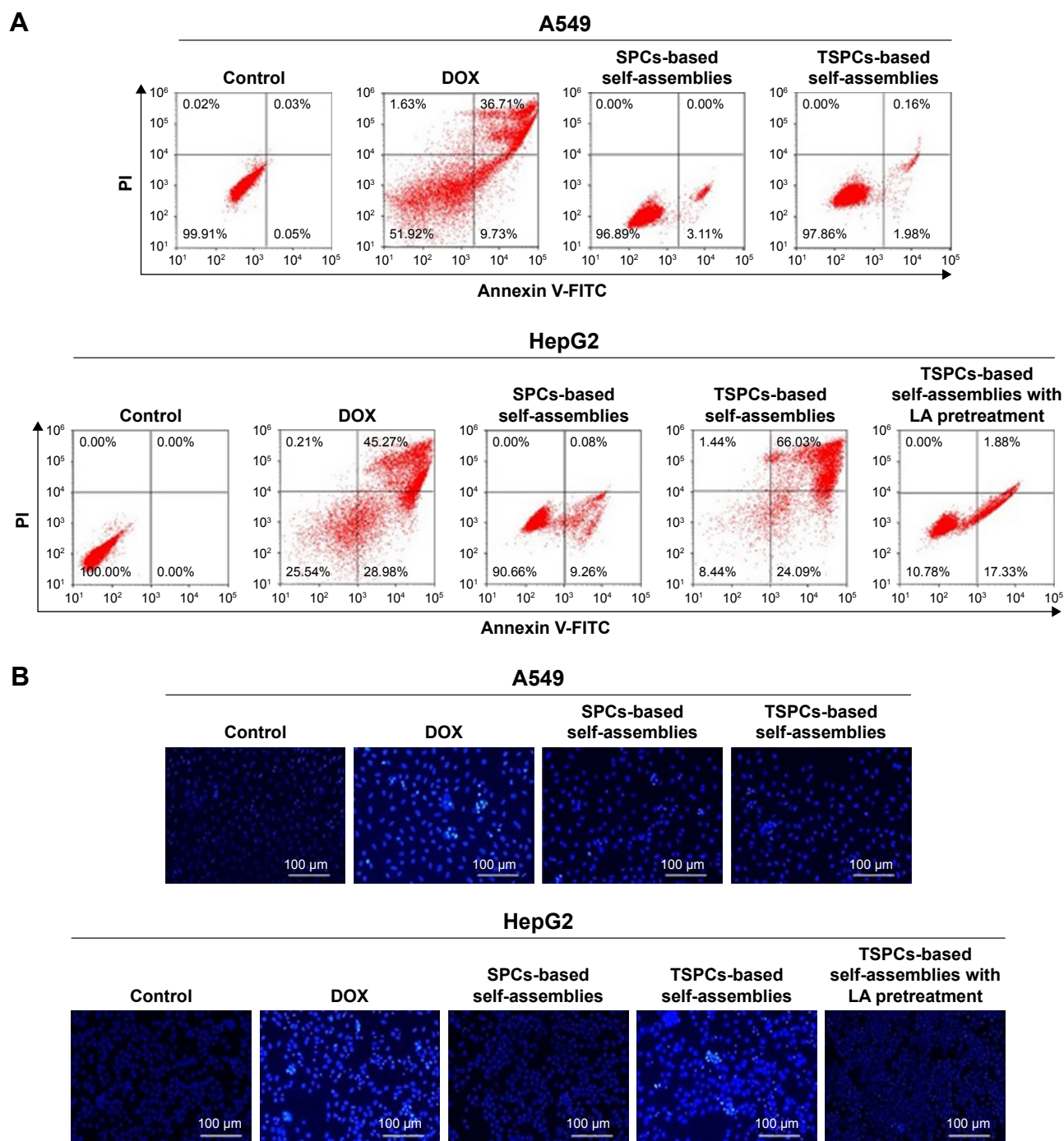


Figure 8 Cell apoptosis analysis of TSPCs- and SPCs-based self-assemblies.

Notes: (A) Cell apoptosis ratio measured by flow cytometry analysis in A549 and HepG2 cells treated with TSPCs- or SPCs-based self-assemblies for 24 hours. (B) Photographs of the morphology of apoptotic nuclei using Hoechst 33258 staining in A549 and HepG2 cells after treatment with TSPCs- or SPCs-based self-assemblies.

Abbreviations: DOX, doxorubicin; LA, lactobionic acid; SPCs, supramolecular prodrug complexes; TSPCs, targeted supramolecular prodrug complexes.

Cell apoptosis analysis of SPCs- and TSPCs-based self-assemblies

Because DOX could induce tumor cells' apoptosis by intercalating with DNA,⁴¹ flow cytometry and Hoechst 33258 staining were carried out. The apoptotic cells were stained with Annexin V. The results (Figure 8A) indicated that after being treated with TSPCs-based self-assemblies for 24 hours, the HepG2 cells' apoptosis rate (right quadrant) was 90.12%, which was a significant increase compared with those treated with SPCs-based self-assemblies (9.45%) or TSPCs-based self-assemblies (19.21%) in the presence of LA. To further confirm these results, Hoechst 33258 staining was carried out to study the nuclear morphology. As depicted in Figure 8B, HepG2 cells treated with free DOX or TSPCs-based self-assemblies for 24 hours, and A549 cells treated with free DOX showed intense blue fluorescence, archetypal of apoptotic cells. At the same time, the condensation of chromatin, shrinkage of nuclei, and condensed bright blue apoptotic nuclei in HepG2 cells were observed only after being treated with free DOX or TSPCs-based self-assemblies for 24 hours. Hence, these data suggest that TSPCs-based self-assemblies were able to induce apoptosis in HepG2 cells.

Conclusion

In summary, we developed biocompatible, pH-sensitive self-assemblies based on host–guest interaction between BM and β -CD for liver cancer therapy. We demonstrated that TSPCs-based self-assemblies have excellent size stability and a well-defined spherical structure. In vitro drug release assay revealed that TSPCs-based self-assemblies, as a pH-sensitive drug carrier, released more drug at pH 5.0 than at the physiological pH value. In vitro cytotoxicity of TSPCs-based self-assemblies was greater than SPCs-based self-assemblies toward HepG2 liver cancer cells. Meanwhile, cell uptake assay proved that the uptake of TSPCs-based self-assemblies was decreased in the presence of LA, which further verified the cell uptake behavior via LA receptors. In addition, the cell apoptosis analysis indicated that TSPCs-based self-assemblies could induce HepG2 cells apoptosis, which may be one of the mechanisms in inhibiting cell proliferation. In conclusion, the DOX-loaded polymers exhibited excellent effects on HCC tumor cell growth, and could potentially be a good candidate to deliver DOX. More importantly, the experimental data we acquired provide a foundation for further in vivo application of DOX-loaded polymers, which offers a strategy for liver cancer-targeting therapy.

Acknowledgments

This work was supported by the National Natural Science Foundation of China (21674086), the Natural Science Basic Research Plan in Shaanxi Province of China (2018JZ2003), the National Natural Science Foundation of China (grant number 81773772), and the Fundamental Research Funds for the Central Universities. Tianfeng Yang and Guowen Du should be regarded as co-first authors. Wei Tian and Yanmin Zhang should be regarded as co-corresponding authors.

Disclosure

The authors report no conflicts of interest in this work.

References

1. Siegel RL, Miller KD, Jemal A. Cancer statistics, 2018. *CA Cancer J Clin*. 2018;68(1):7–30.
2. Moukhaider HM, Halawi R, Cappellini MD, Taher AT. Hepatocellular carcinoma as an emerging morbidity in the thalassemia syndromes: a comprehensive review. *Cancer*. 2017;123(5):751–758.
3. Li Y, Zhu D, Hou L, et al. TRB3 reverses chemotherapy resistance and mediates crosstalk between endoplasmic reticulum stress and AKT signaling pathways in MHCC97H human hepatocellular carcinoma cells. *Oncol Lett*. 2018;15(1):1343–1349.
4. Wang W, Peng H, Li J, et al. Controllable inhibition of hepatitis B virus replication by a DR1-targeting short hairpin RNA (shRNA) expressed from a DOX-inducible lentiviral vector. *Virus Genes*. 2013;46(3):393–403.
5. Kebba W, Lahouel M, Rouibah H, et al. Reversing multidrug resistance in chemo-resistant human lung adenocarcinoma (A549/DOX) cells by Algerian propolis through direct inhibiting the Pgp efflux-pump, G0/G1 cell cycle arrest and apoptosis induction. *Anticancer Agents Med Chem*. 2018;18(9):1330–1337.
6. Bertrand N, Wu J, Xu X, Kamaly N, Farokhzad OC. Cancer nanotechnology: the impact of passive and active targeting in the era of modern cancer biology. *Adv Drug Deliv Rev*. 2014;66:2–25.
7. Cong Z, Shi Y, Wang Y, et al. A novel controlled drug delivery system based on alginate hydrogel/chitosan micelle composites. *Int J Biol Macromol*. 2018;107(Pt A):855–864.
8. Li S, Goins B, Zhang L, Bao A. Novel multifunctional theranostic liposome drug delivery system: construction, characterization, and multimodality MR, near-infrared fluorescent, and nuclear imaging. *Bioconjug Chem*. 2012;23(6):1322–1332.
9. Ye J, Shin MC, Liang Q, He H, Yang VC. 15 years of ATTEMPTS: a macromolecular drug delivery system based on the CPP-mediated intracellular drug delivery and antibody targeting. *J Control Release*. 2015;205:58–69.
10. Dave V, Yadav RB, Kushwaha K, et al. Lipid-polymer hybrid nanoparticles: Development & statistical optimization of norfloxacin for topical drug delivery system. *Bioact Mater*. 2017;2(4):269–280.
11. Rossi F, Ferrari R, Castiglione F, et al. Polymer hydrogel functionalized with biodegradable nanoparticles as composite system for controlled drug delivery. *Nanotechnology*. 2015;26(1):015602.
12. Soltani Y, Goodarzi N, Mahjub R. Preparation and characterization of self nano-emulsifying drug delivery system (SNEDDS) for oral delivery of heparin using hydrophobic complexation by cationic polymer of β -cyclodextrin. *Drug Dev Ind Pharm*. 2017;43(11):1899–1907.
13. Liu G, Yuan Q, Hollett G, et al. Cyclodextrin-based host–guest supramolecular hydrogel and its application in biomedical fields. *Polym Chem*. 2018;9(25):3436–3449.
14. Wang XG, Dong ZY, Cheng H, et al. A multifunctional metal-organic framework based tumor targeting drug delivery system for cancer therapy. *Nanoscale*. 2015;7(38):16061–16070.

15. Yu F, Wu H, Tang Y, et al. Temperature-sensitive copolymer-coated fluorescent mesoporous silica nanoparticles as a reactive oxygen species activated drug delivery system. *Int J Pharm*. 2018;536(1):11–20.
16. Dabiri SMH, Lagazzo A, Barberis F, et al. New in-situ synthesized hydrogel composite based on alginate and brushite as a potential pH sensitive drug delivery system. *Carbohydr Polym*. 2017;177:324–333.
17. Papa AL, Korin N, Kanapathipillai M, et al. Ultrasound-sensitive nanoparticle aggregates for targeted drug delivery. *Biomaterials*. 2017; 139:187–194.
18. Zuo J, Tu L, Li Q, et al. Near Infrared Light Sensitive Ultraviolet-Blue Nanophotoswitch for Imaging-Guided “Off-On” Therapy. *ACS Nano*. 2018;12(4):3217–3225.
19. Chen B, Dai W, He B, et al. Current multistage drug delivery systems based on the tumor microenvironment. *Theranostics*. 2017;7(3):538–558.
20. Butt AM, Amin MC, Katas H, et al. Doxorubicin and siRNA Codelivery via chitosan-coated pH-responsive mixed micellar polyplexes for enhanced cancer therapy in multidrug-resistant tumors. *Mol Pharm*. 2016;13(12):4179–4190.
21. Ak G, Yilmaz H, Güneş A, Hamarat Sanlier S. In vitro and in vivo evaluation of folate receptor-targeted a novel magnetic drug delivery system for ovarian cancer therapy. *Artif Cells Nanomed Biotechnol*. 2018;46(sup1):926–937.
22. Jung KH, Park JW, Paik JY, et al. EGF receptor targeted tumor imaging with biotin-PEG-EGF linked to (99m)Tc-HYNIC labeled avidin and streptavidin. *Nucl Med Biol*. 2012;39(8):1122–1127.
23. Roggenbuck D, Mytilinaiou MG, Lapin SV, Reinhold D, Conrad K. Asialoglycoprotein receptor (ASGPR): a peculiar target of liver-specific autoimmunity. *Auto Immun Highlights*. 2012;3(3):119–125.
24. Wang X, He L, Wei B, et al. Bromelain-immobilized and lactobionic acid-modified chitosan nanoparticles for enhanced drug penetration in tumor tissues. *Int J Biol Macromol*. 2018;115:129–142.
25. Bansal D, Yadav K, Pandey V, et al. Lactobionic acid coupled liposomes: an innovative strategy for targeting hepatocellular carcinoma. *Drug Deliv*. 2016;23(1):140–146.
26. Sonawane SJ, Kalhapure RS, Govender T. Hydrazone linkages in pH responsive drug delivery systems. *Eur J Pharm Sci*. 2017;99:45–65.
27. Xu ZG, Zhang KL, Hou CL, et al. A novel nanoassembled doxorubicin prodrug with a high drug loading for anticancer drug delivery. *J Mater Chem B*. 2014;2(22):3433–3437.
28. Zhang Z, Ding J, Chen X, et al. Intracellular pH-sensitive supramolecular amphiphiles based on host–guest recognition between benzimidazole and β -cyclodextrin as potential drug delivery vehicles. *Polym Chem*. 2013;4(11):3265.
29. Zhao Y, Fan Z, Shen M, Shi X, et al. Capturing hepatocellular carcinoma cells using lactobionic acid-functionalized electrospun polyvinyl alcohol/polyethyleneimine nanofibers. *RSC Adv*. 2015;5(86):70439–70447.
30. Chipem FA, Behera SK, Krishnamoorthy G. Enhancing excited state intramolecular proton transfer in 2-(2'-hydroxyphenyl)benzimidazole and its nitrogen-substituted analogues by β -cyclodextrin: the effect of nitrogen substitution. *J Phys Chem A*. 2013;117(20):4084–4095.
31. Ma H, Wang Y, Wu D, et al. A novel controlled release immunosensor based on benzimidazole functionalized SiO₂ and cyclodextrin functionalized gold. *Sci Rep*. 2016;6:19797.
32. Gao L, Zheng B, Chen W, Schalley CA. Enzyme-responsive pillar[5] arene-based polymer-substituted amphiphiles: synthesis, self-assembly in water, and application in controlled drug release. *Chem Commun*. 2015;51(80):14901–14904.
33. Stephenson A, Wu Z, Yuan X. The preformulation stability studies of a proline prodrug of methotrexate. *Med Chem*. 2012;8(4):622–628.
34. Di-Wen S, Pan GZ, Hao L, et al. Improved antitumor activity of epirubicin-loaded CXCR4-targeted polymeric nanoparticles in liver cancers. *Int J Pharm*. 2016;500(1–2):54–61.
35. Gao GH, Li Y, Lee DS. Environmental pH-sensitive polymeric micelles for cancer diagnosis and targeted therapy. *J Control Release*. 2013; 169(3):180–184.
36. Zhan F, Chen W, Wang Z, et al. Acid-activatable prodrug nanogels for efficient intracellular doxorubicin release. *Biomacromolecules*. 2011; 12(10):3612–3620.
37. Wang L, Ren KF, Wang HB, Wang Y, Ji J. pH-sensitive controlled release of doxorubicin from polyelectrolyte multilayers. *Colloids Surf B Biointerfaces*. 2015;125:127–133.
38. Siepmann J, Peppas NA. Modeling of drug release from delivery systems based on hydroxypropyl methylcellulose (HPMC). *Adv Drug Delivery Rev*. 2001;48(2–3):139–157.
39. Yang X, Grailer JJ, Pilla S, Steeber DA, Gong S, et al. Tumor-targeting, pH-responsive, and stable unimolecular micelles as drug nanocarriers for targeted cancer therapy. *Bioconjug Chem*. 2010;21(3):496–504.
40. Zakeri-Milani P, Mussa Farkhani S, Shirani A, et al. Cellular uptake and anti-tumor activity of gemcitabine conjugated with new amphiphilic cell penetrating peptides. *EXCLI J*. 2017;16:650–662.
41. Hajra S, Patra AR, Basu A, Bhattacharya S. Prevention of doxorubicin (DOX)-induced genotoxicity and cardiotoxicity: Effect of plant derived small molecule indole-3-carbinol (I3C) on oxidative stress and inflammation. *Biomed Pharmacother*. 2018;101:228–243.

International Journal of Nanomedicine

Publish your work in this journal

The International Journal of Nanomedicine is an international, peer-reviewed journal focusing on the application of nanotechnology in diagnostics, therapeutics, and drug delivery systems throughout the biomedical field. This journal is indexed on PubMed Central, MedLine, CAS, SciSearch®, Current Contents®/Clinical Medicine,

Submit your manuscript here: <http://www.dovepress.com/international-journal-of-nanomedicine-journal>

Dovepress

Journal Citation Reports/Science Edition, EMBASE, Scopus and the Elsevier Bibliographic databases. The manuscript management system is completely online and includes a very quick and fair peer-review system, which is all easy to use. Visit <http://www.dovepress.com/testimonials.php> to read real quotes from published authors.